

Stamping Patterns of Insulated Gold Nanowires with Self-Organized Ultrathin Polymer Films

James M. Helt,^{*,†} Charles Michael Drain,^{*,‡} and Giorgio Bazzan[‡]

Contribution from the Department of Chemistry, College of Staten Island and the Graduate Center of the City University of New York, 2800 Victory Boulevard, Staten Island, New York 10314, and Department of Chemistry and Biochemistry, Hunter College and the Graduate Center of the City University of New York, 695 Park Avenue, New York, New York 10021

Received October 5, 2005; Revised Manuscript Received May 26, 2006; E-mail: cdrain@hunter.cuny.edu; jhelt275@yahoo.com

Abstract: A thermal contact transfer technique is presented for the fabrication of nanoscaled to microscaled patterns of polymer-insulated metal structures on ceramic surfaces using metal-coated, thermoplastic stamps. The thermally activated formation of polymer-metal-polymer (PMP) heterostructures occurs spontaneously when a metal-coated thermoplastic stamp is compressed against a ceramic substrate and subsequently heated. The presented technique exploits the dynamics of ultrathin polymer films localized at interfaces and interfacial forces to prompt local reorganization of polymer stamp materials during processing. Intercalation of polymer stamp materials into the metal-substrate interface yields a cohesive polymer layer that binds the metal layer to the substrate. Disproportionate adhesion between the bulk polymer and the polymer layer at the stamp-metal interface leaves a capping layer upon separation of the stamp from the substrate. Here we demonstrate this technique with single use, bilevel polymer stamps which afford transfer of two distinct general products. The transfer of insulated submicrometer wide wires from the *raised* stamp features affords patterns of trilayered PMP structures with uniform wire dimensions. Concomitant transfer from the *recessed* stamp features allows fabrication of multilayered PMP architectures with sub-100 nm spacing from microstructured polymer stamps. Thus, patterns with two different insulated nanowire widths are readily fabricated in a single stamping process. A variety of ceramic substrates, thermoplastic materials, and metals can be used; e.g., inexpensive gold-coated CD or DVD media can be used as stamps, where the combination of materials dictates the relative interfacial forces and the processing parameters.

Introduction

The miniaturization of electronics, sensors, displays, and other functional devices has driven intense research and development into new methods to form arrays of nanostructured features on surfaces. Often, these applications require complex patterns of features with multiple layers and multiple dimensions. There are a variety of lithographic approaches available for the formation of nanostructured materials on surfaces that, similar to those used in the fine arts, can be divided into subtractive and additive methods.^{1,2} Subtractive methods are typified by the use of masks or stencils and electromagnetic radiation to systematically etch or chemically alter components of a blank that is comprised of various material layers with appropriate properties for the final nanoscaled device or structure. These subtractive processes are the progeny of photolithographic methods such as blue printing, wherein a mask covers the paper substrate impregnated with two iron complexes and light initiates

the formation of an insoluble Prussian blue and water removes the un-reacted salts. Subtractive methods are well-developed, quite versatile, and are capable of creating structures that are ~10 nm wide to those that are many microns wide. Additive methods are typified by the use of patterned stamps bearing materials, usually on the raised features, which can be transferred to an appropriate substrate by the differences in adhesive forces among the material, the stamp, and the substrate. Exemplary stamping techniques are capable of generating structures down to ca. 10 nm wide but are generally limited to the parallel transfer of one material at a time.¹ Stamps descend from lithography wherein a pattern of an oily ink surrounded by a film of water is transferred to paper by the greater affinity of the ink to the paper than to the substrate. The use of AFM tips to engrave (nanoshaving)³ and write (dip pen)⁴ nanoscaled patterns are also available and are analogous to hand-drawing.

In terms of soft lithographic techniques,⁵⁻⁷ these include microcontact printing,⁸⁻¹⁵ nanoimprint lithography,¹⁶⁻²⁴ soft molding,²⁵ reverse nanoimprint lithography,²⁶ laser-assisted direct imprint,²⁷ cold welding nanotransfer,^{28,29} lithography

[†] College of Staten Island and the Graduate Center of the City University of New York.

[‡] Hunter College and the Graduate Center of the City University of New York.

(1) *Adv. Mater.* **2004**, *16*, 1235-1378.

(2) Gates, B. D. *Materials Today* **2005**, *8*, 44-49.

(3) Liu, G. Y.; Xu, S.; Qian, Y. L. *Acc. Chem. Res.* **2000**, *33*, 457-466.

(4) Piner, R. D.; Zhu, J.; Xu, F.; Hong, S.; Mirkin, C. A. *Science* **1999**, *283*, 661-663.

controlled wetting,³⁰ superlattice nanowire pattern transfer,³¹ nanotransfer printing,^{32–35} molecular transfer lithography,³⁶ and micromolding in capillaries.^{37–40} We recently reported a chemical–mechanical method, which utilizes micromolded polymer stamps, for the synthesis and transfer of materials (e.g., malleable metals) to and from polymers.⁴¹ This chemical–mechanical method, for example, allows the fabrication of complex patterns of gold nanowires (and other structures) on either polymer or ceramic supports. The processing parameters of each of these replica-based stamping methods dictate the types of materials that can be used and the structures that can be fabricated. Therefore, this array of soft lithographic methods enables the fabrication of nanoscaled patterns of a variety of materials on a variety of surfaces. In general with most soft lithographic methods, a single stamping/imprinting affords patterns of a single material in two dimensions, which necessitates additional (sequential) procedures to fabricate multilayer heterostructured arrays.

We now demonstrate that the unique behavior of ultrathin polymer films provides another element of tailorability that can be exploited to pattern arrays of self-aligned micro- to nanoscale

heterostructures on ceramic surfaces. The soft lithography technique reported here beneficially exploits finite size effects of confined polymer films for the fabrication of multilayered polymer–metal–polymer (PMP) heterostructures on ceramic surfaces. The technique involves multilayer thermal nanotransfer. The thermal nanotransfer of polymer–metal heterostructures detailed here enables direct fabrication of multilayer architectures in a rapid, parallel fashion without employing advanced lithographic tooling or “wet” chemistry for pattern development. Numerous multilayer architectures are available with this method, and the potential exists for the fabricated structures and/or substrate to be processed further with conventional and advanced lithographic techniques (e.g., etching, UV–visible photolithography, e-beam and X-ray lithography).

The formation of nanostructured arrays of thermoplastic materials on substrates, using liquid monomers that are later polymerized or solid plastic “inks”, has been reported.^{2,26,42–52} Allyl monomers can be used in nanoimprint lithography as heating during the imprint process cures the polymer.⁴³ Capillary forces can be exploited to place polymer solutions into recessed stamp features,⁴² and for nanoimprint methods of thin films.^{44,53} The squeezed flow of polymers into cavities has been modeled and demonstrated.⁴⁵ Some polymers have been doped with fluorescent dyes to form solid-state dye lasers.⁵⁴ Enabled by differential wetting/dewetting, patterns of thin polystyrene (PS) films on chemically patterned substrates has been demonstrated,⁴⁶ and the transfer of polymers from molds to substrates has also been discussed.²⁶ The processes wherein a solid polymer is transferred from the stamp to a substrate have some relevance to the processes described herein in that they both exploit wetting/dewetting dynamics⁵⁵ and the unique properties of interfacial polymer films (see below). The use of interfacial forces for such purposes has been succinctly illustrated by both the soft lithographic transfer techniques^{56,57} and recent developments in organic display fabrication technology.^{58,59} The insulated gold wires presented here are unique in

- (5) Christenson, H. K. *J. Phys. Chem.* **1993**, *97*, 12034–12041.
- (6) Xia, Y. N.; Rogers, J. A.; Paul, K. E.; Whitesides, G. M. *Chem. Rev.* **1999**, *99*, 1823–1848.
- (7) Gates, B. D.; Xu, Q.; Stewart, M.; Ryan, D.; Willson, C. G.; Whitesides, G. M. *Chem. Rev.* **2005**, *105*, 1171–1196.
- (8) Goetting, L. B.; Deng, T.; Whitesides, G. M. *Langmuir* **1999**, *15*, 1182–1191.
- (9) Michel, B.; Bernard, A.; Bietsch, A.; Delamarche, E.; Geissler, M.; Juncker, D.; Kind, H.; Renault, J. P.; Rothuizen, H.; Schmid, H.; Schmidt-Winkel, P.; Stutz, R.; Wolf, H. *IBM Journal of Research and Development* **2001**, *45*, 697–719.
- (10) Ng, W. K.; Wu, L.; Moran, P. M. *Appl. Phys. Lett.* **2002**, *81*, 3097–3099.
- (11) Zhong, Z. Y.; Gates, B.; Xia, Y. N.; Qin, D. *Langmuir* **2000**, *16*, 10369–10375.
- (12) Kumar, A.; Whitesides, G. M. *Appl. Phys. Lett.* **1993**, *63*, 2002–2004.
- (13) Schmid, H.; Michel, B. *Macromolecules* **2000**, *33*, 3042–3049.
- (14) Moran, C. E.; Radloff, C.; Halas, N. J. *Adv. Mater.* **2003**, *15*, 804–807.
- (15) St. John, P. M.; Craighhead, H. G. *Appl. Phys. Lett.* **1996**, *68*, 1022–1024.
- (16) Chou, S. Y.; Krauss, P. R.; Renstrom, P. J. *Appl. Phys. Lett.* **1995**, *67*, 3114–3116.
- (17) Chou, S. Y.; Krauss, P. R.; Renstrom, P. J. *J. Vac. Sci. Technol., B* **1996**, *14*, 4129–4133.
- (18) Chou, S. Y.; Krauss, P. R.; Renstrom, P. J. *Science* **1996**, *272*, 85–87.
- (19) Krauss, P. R.; Chou, S. Y. *Appl. Phys. Lett.* **1997**, *71*, 3174–3176.
- (20) Li, M. T.; Chen, L.; Chou, S. Y. *Appl. Phys. Lett.* **2001**, *78*, 3322–3324.
- (21) Austin, M. D.; Chou, S. Y. *Appl. Phys. Lett.* **2002**, *81*, 4431–4433.
- (22) Cao, H.; Yu, Z. N.; Wang, J.; Tegenfeldt, J. O.; Austin, R. H.; Chen, E.; Wu, W.; Chou, S. Y. *Appl. Phys. Lett.* **2002**, *81*, 174–176.
- (23) Austin, M.; Chou, S. Y. *J. Vac. Sci. Technol., B* **2002**, *20*, 665–667.
- (24) Wu, W.; Cui, B.; Sun, X. Y.; Zhang, W.; Zhuang, L.; Kong, L. S.; Chou, S. Y. *J. Vac. Sci. Technol., B* **1998**, *16*, 3825–3829.
- (25) Kim, Y. S.; Park, J.; Lee, H. *Appl. Phys. Lett.* **2002**, *81*, 1011–1013.
- (26) Huang, X. D.; Bao, L. R.; Cheng, X.; Guo, L. J.; Pang, S. W.; Yee, A. F. *J. Vac. Sci. Technol., B* **2002**, *20*, 2872–2876.
- (27) Chou, S. Y.; Keimel, C.; Gu, J. *Nature* **2002**, *417*, 835–837.
- (28) Kim, C.; Forrest, S. R. *Adv. Mater.* **2003**, *15*, 541–545.
- (29) Kim, C.; Shtein, M.; Forrest, S. R. *Appl. Phys. Lett.* **2002**, *80*, 4051–4053.
- (30) Cavallini, M.; Biscarini, F. *Nano Lett.* **2003**, *3*, 1269–1271.
- (31) Melosh, N. A.; Boukai, A.; Diana, F.; Gerardot, B.; Badolato, A.; Petroff, P. M.; Heath, J. R. *Science* **2003**, *300*, 112–115.
- (32) Zaumseil, J.; Meitl, M. A.; Hsu, J. W. P.; Acharya, B. R.; Baldwin, K. W.; Loo, Y. L.; Rogers, J. A. *Nano Lett.* **2003**, *3*, 1223–1227.
- (33) Loo, Y. L.; Willett, R. L.; Baldwin, K. W.; Rogers, J. A. *J. Am. Chem. Soc.* **2002**, *124*, 7654–7655.
- (34) Loo, Y. L.; Willett, R. L.; Baldwin, K. W.; Rogers, J. A. *Appl. Phys. Lett.* **2002**, *81*, 562–564.
- (35) Matsui, S.; Igaku, Y.; Ishigaki, H.; Fujita, J.; Ishida, M.; Ochiai, Y.; Namatsu, H.; Komuro, M. *J. Vac. Sci. Technol., B* **2003**, *21*, 688–692.
- (36) Schaper, C. D. *Nano Lett.* **2003**, *3*, 1305–1309.
- (37) Kim, E.; Xia, Y. N.; Whitesides, G. M. *Nature* **1995**, *376*, 581–584.
- (38) Kim, E.; Xia, Y. N.; Whitesides, G. M. *J. Am. Chem. Soc.* **1996**, *118*, 8, 5722–5731.
- (39) Pisignano, D.; Sariconi, E.; Mazzeo, M.; Gigli, G.; Cingolani, R. *Adv. Mater.* **2002**, *14*, 1565–1567.
- (40) Xia, Y. N.; Kim, E.; Whitesides, G. M. *Chem. Mater.* **1996**, *8*, 1558–1567.
- (41) Helt, J. M.; Drain, C. M.; Battaes, J. D. *J. Am. Chem. Soc.* **2004**, *126*, 628–634.
- (42) Salleo, A.; Wong, W. S.; Chabincyn, M. L.; Paul, K. E.; Street, R. A. *Adv. Funct. Mater.* **2005**, *15*, 1105–1110.
- (43) Reuther, F.; Kubenz, M.; Schuster, C.; Fink, M.; Vogler, M.; Gruetzner, G.; Grimm, J.; Kaepfel, A. In *Emerging Lithographic Technologies IX*; Mackay, R. S., Ed.; SPIE: San Jose, CA, 2005; Vol. 5751, pp 976–985.
- (44) Kehagias, N.; Zelsmann, M.; Torres, C. M. S. In *Opto-Ireland 2005: Optoelectronics, Photonic Devices, and Optical Networks*; McInerney, J. G.; Farrell, G.; Denieffe, D. M.; Barry, L. P.; Gamble, H. S.; Hughes, P. J.; Moore, A., Eds.; SPIE: Dublin, Ireland, 2005; Vol. 5825, pp 654–660.
- (45) Bogdanskii, N.; Wissen, M.; Ziegler, A.; Scheer, H.-C. *Microelectronic Engineering* **2005**, *78–79*, 598–604.
- (46) Zhang, Z.; Wang, Z.; Xing, R.; Han, Y. *Polymer* **2003**, *44*, 3737–3743.
- (47) Suh, K. Y.; Langer, R. *Appl. Phys. Lett.* **2003**, *83*, 1668–1670.
- (48) Gourdin, S.; Hammond, P.; Crites, T.; Coe, S.; Bulovic, V. In *Materials Research Society Symposium D – Proceedings*; Shur, M. S.; Wilson, P. M.; Urban, D., Eds.; MRS: 2002; Vol. 736, pp 271–276.
- (49) Meitl, M. A.; Zhu, Z. T.; Lee, K. J.; Nuzzo, R. G.; Rogers, J. A.; Kumar, V.; Adesida, I.; Feng, X.; Huang, Y. Y. *Nature Materials* **2006**, *5*, 33–38.
- (50) Rogers, J. A.; Nuzzo, R. G. *Materials Today* **2005**, *8*, 50–56.
- (51) Nielsen, T.; Pedersen, R. H.; Hansen, O.; Kristensen, A.; Haatainen, T.; Tolkki, A.; Ahopelto, J. In *Technical Digest of the 18th IEEE Conference on Micro Electro Mechanical Systems, MEMS 2005*; Miami, FL, 2005; pp 508–511.
- (52) Kee, C. S.; Yoon, K. B.; Choi, C. G. I.; Kim, J. T.; Han, S. P.; Park, S.; Schiff, H. J. *Nonlinear Opt. Phys. Mater.* **2005**, *14*, 299–303.
- (53) Menard, E.; Bilhaut, L.; Zaumseil, J.; Rogers, J. A. *Langmuir* **2004**, *20*, 6871–6878.
- (54) Nilsson, D.; Nielsen, T.; Kristensen, A. *Rev. Sci. Instrum.* **2004**, *75*, 4481–4486.
- (55) de Gennes, P. G. *Rev. Mod. Phys.* **1985**, *57*, 827–863.
- (56) Ahn, H.; Lee, K. J.; Shim, A.; Rogers, J. A.; Nuzzo, R. G. *Nano Lett.* **2005**, *5*, 2533–2537.
- (57) Childs, W. R.; Motala, M. J.; Lee, K. J.; Nuzzo, R. G. *Langmuir* **2005**, *21*, 10096–10105.
- (58) Lee, J. Y.; Lee, S. T. *Adv. Mater.* **2004**, *16*, 51–54.

that a single processing step yields a product with three distinct layers (PMP structures) with submicrometer dimensions.

The formation of micron to nanometer scale arrays of insulated gold heterostructures is enabled by the physics of ultrathin polymer films and differential adhesion forces arising from polymer reorganization at the stamp–gold film interface. Since the seminal work of Cory, Keddle, and Jones,^{60,61} numerous studies have examined the thermophysical properties of ultrathin films, e.g., the glass transition temperature (T_g) and expansivity, and the general conclusion is that as the film thickness (h) approaches scales on the order of the macromolecule's radius of gyration (R_g), the film's physical properties diverge significantly from that of the bulk.^{62–70} This dimensional dependence of the thermoplastic properties of polymers at interfaces is key to existing and future polymer technologies that exploit the fundamental performance capabilities of these materials. For example, the wetting/dewetting, friction, adhesion, and fracture properties of polymers will continue to be tested as they serve critical functions in coatings, lubricants,⁷¹ and emerging technologies such as nanoimprint lithography¹⁶ and data storage.⁷²

The thermal nanotransfer of polymer–metal–polymer heterostructures exploits the unique cooperative self-organizational properties of polymers at interfaces described above.⁶² Figure 1 illustrates the steps employed in the method discussed here: (1) a thermoplastic polymer stamp is coated with a discontinuous thin film material (e.g. gold) to be transferred to the substrate; and (2) the coated polymer stamp is compressed against a substrate, briefly heated, and subsequently separated from the substrate after cooling. From a single polymer stamp this process enables fabrication of two distinct nanostructured PMP products, Figure 1b and c, through transfer of both the thin film and a portion of the outermost surface of the polymer stamp to the substrate. The resulting architecture of the PMP structures depends on both the initial stamp geometry (i.e., relating to the number of topologically unique raised and recessed stamp features), as well as processing parameters (e.g., applied load, processing time, and temperature; see Supporting Information). The polymer stamp depicted in Figure 1 possesses a “bilevel” architecture, where each stamp level is defined by the relative stamp feature height—raised and recessed. The final pattern of the fabricated multilayer arrays on the substrate correspond to

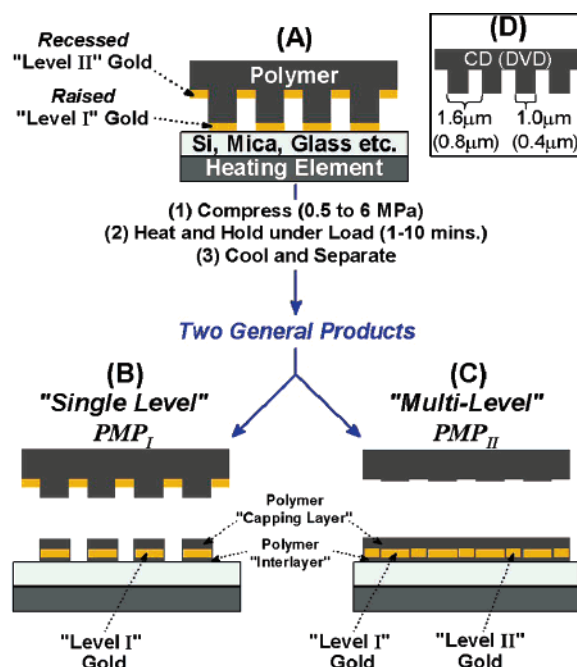


Figure 1. Schematic of the multilayer thermal nanotransfer process where polymer–metal heterostructures are fabricated from a bilevel polymer stamp coated with a thin Au film. The coated polymer stamp is brought into compressive contact with a substrate (e.g., mica, glass, silicon, ITO) and subsequently heated ($-45\text{ }^{\circ}\text{C} < T_g < 10\text{ }^{\circ}\text{C}$). Depending on the applied load, duration of heating, and the soak temperature, two general trilayer products can be formed on the substrate. In both instances the trilayer structure is comprised of a polymer interlayer, a Au film layer, and a polymer capping layer. (b) Depicts the PMP_I product, where only the Au and polymer from the “raised” portion of the polymer stamp are transferred to the substrate (termed a single-level transfer). (c) Depicts the PMP_{II} product, where Au and polymer from both the raised and recessed stamp features are transferred to the substrate (termed a “multilevel” transfer). (d) Depicts the repeat grating structure of commercial CD and DVD stamps, which possess a recess depth of $\sim 150\text{--}200\text{ nm}$.

the initial stamp geometry and, thereby, falls into two general categories: (1) material is transferred *only* from the raised stamp features (termed a single-level transfer), corresponding to PMP_I products (Figure 1b); and (2) material is transferred from *both* the raised and recessed stamp features (termed a “multilevel” transfer), corresponding to PMP_{II} products (Figure 1c). In general, structures fabricated with polycarbonate stamps on mica, oxidized silicon wafers, and indium tin oxide substrates have a trilayer architecture with (1) an ultrathin polymer interlayer that has diffused and intercalated into the metal–substrate interface, (2) a metal film layer (e.g., gold), and (3) a polymer capping layer that coats the metal film.

In terms of a general mechanism, the observed multilayer formation and transfer is enabled by several phenomena acting in concert including the unique interfacial properties of ultrathin polymer films.^{60–70,73} Qualitatively, this may be described further according to the final multilayer product: (1) the spreading and self-organization of the polymer interlayer, (2) the formation of a polymer–polymer “interface” between the capping layer and the bulk stamp, and (3) cohesive failure at the polymer–polymer “interface” between the capping layer and the bulk stamp. The spontaneous self-organization of the interlayer can be understood in terms of wetting phenomena and the spreading of an ultrathin polymer precursor film on the

- (59) Chin, B. D.; Suh, M. C.; Kim, M. H.; Kang, T. M.; Yang, N. C.; Song, M. W.; Lee, S. T.; Kwon, J. H.; Chung, H. K.; Wolk, M. B.; Bellmann, E.; Baetzold, J. P. *J. Information Display* **2003**, *4*, 1–5.
 (60) Keddle, J. L.; Jones, R. A. L.; Cory, R. A. *Europhysics Lett.* **1994**, *27*, 59–64.
 (61) Keddle, J. L.; Jones, R. A. L.; Cory, R. A. *Faraday Discussions* **1994**, *219–230*.
 (62) Ellison, C. J.; Torkelson, J. M. *Nature Materials* **2003**, *2*, 695–700.
 (63) Forrest, J. A.; Dalnoki-Veress, K.; Stevens, J. R.; Dutcher, J. R. *Phys. Rev. Lett.* **1996**, *77*, 2002–2005.
 (64) Forrest, J. A.; Dalnoki-Veress, K. *Adv. Colloid Interface Sci.* **2001**, *94*, 167–196.
 (65) Fukao, K.; Miyamoto, Y. *Phys. Rev. E* **2000**, *61*, 1743–1754.
 (66) Kawana, S.; Jones, R. A. L. *Phys. Rev. E* **2001**, *63*, 021501.
 (67) Sharp, J. S.; Teichroeb, J. H.; Forrest, J. A. *Eur. Phys. J. E* **2004**, *15*, 473–487.
 (68) Soles, C. L.; Douglas, J. F.; Jones, R. L.; Wu, W. *Macromolecules* **2004**, *37*, 2901–2908.
 (69) Soles, C. L.; Douglas, J. F.; Wu, W. L.; Peng, H.; Gidley, D. W. *Macromolecules* **2004**, *37*, 2890–2900.
 (70) Tseng, K. C.; Turro, N. J.; Durning, C. J. *Phys. Rev. E* **2000**, *61*, 1800–1811.
 (71) *Springer Handbook of Nanotechnology*; Bhushan, B., Ed.; Springer: Berlin, 2004; p 1222.
 (72) Durig, U.; Cross, G.; Despont, M.; Drechsler, U.; Haberler, W.; Lutwyche, M. I.; Rothuizen, H.; Stutz, R.; Widmer, R.; Vettiger, P.; Binnig, G. K.; King, W. P.; Goodson, K. E. *Tribology Letters* **2000**, *9*, 25–32.

- (73) DeMaggio, G. B.; Frieze, W. E.; Gidley, D. W.; Zhu, M.; Hristov, H. A.; Yee, A. F. *Phys. Rev. Lett.* **1997**, *78*, 1524–1527.

high surface energy metal ($\gamma_{\text{gold}} \sim 1800 \text{ mN/m}$ at $145 \text{ }^\circ\text{C}$)^{74,75} and substrate ($\gamma_{\text{mica}} \sim 144 \text{ mN/m}$)⁵ surfaces. Such favorable interfacial interactions promote intercalation of polymer stamp materials into the metal–substrate interface. This ultrathin polymer interlayer is an integral component of this transfer process as it acts to bind the metal film to the substrate and, therefore, must be sufficiently robust to withstand the tensile forces exerted during stamp–substrate separation.⁷⁶ Retention of the multilayer structures by the substrate is also a consequence of cohesive failure at the capping layer–stamp “interface”. In light of the fact that the capping layer and stamp are compositionally the same polymeric material, it is surprising that adhesive failure would preferentially occur at this interface rather than at the substrate–interlayer interface. There are several possible explanations for this cohesive failure, with the most intriguing centered on the developing description of ultrathin films of polymers introduced above.⁷⁷ One proposal suggests that confined polymer films possess a three-layered architecture comprised of “dead”, “bulk”, and a “liquidlike” layer at an interface.^{60,61,65,66,73} The molecular properties that give rise to these three phases are still under discussion. However, this model could account for the observed formation of both the interlayer and the capping polymer layer of the PMP product, provided that cohesive anisotropies exist between the three layers. The question of which specific properties are accountable for this anisotropy is difficult to ascertain at this point; however, a number of effects are likely acting cooperatively (e.g., thermal expansion mismatch, dewetting, density gradients,⁶² and entanglement variations between each layer). Structural analysis of the multilayer PMP products presented below provides evidence for the role of cohesive anisotropies in thin polymer film systems.

Single-Level Transfer: PMP₁ Microstructure Fabrication.

We have evaluated the multilayer thermal nanotransfer of polymer–metal heterostructures using a number of polycarbonate (PC) stamps. Figure 2 illustrates the products of a single-level transfer to a mica substrate employing a compression molded polycarbonate stamp (Lexan, M_w 24 kg/mol by GPC, PDI ~ 2.1 ; $T_g = 151 \text{ }^\circ\text{C}$, nominal unperturbed $R_g \sim 7.1 \text{ nm}$ ^{78,79}). Lexan stamps possessed a minimum feature width $\sim 5 \text{ }\mu\text{m}$ and a 500 nm recess depth. Here the PC stamp was coated with a 10 nm Au film and processed at $145 \text{ }^\circ\text{C}$ for 1 min under an applied pressure of $\sim 0.9 \text{ MPa}$. Due to the wide range of sub- T_g processing temperatures, it is important to note that the processing times stated herein only account for the time spent at the soak temperature (the soak time and temperature refer to the period in which the stamp is held at constant temperature) and does not include the time required to heat and cool the sample. Typically it takes $\sim 2 \text{ min}$ for the aluminum heating plate to heat from $45 \text{ }^\circ\text{C}$ to $145 \text{ }^\circ\text{C}$ and approximately 2 min to cool from $145 \text{ }^\circ\text{C}$ to $100 \text{ }^\circ\text{C}$. More details on the thermal history (i.e., a typical temperature program) are described in the Supporting Information.

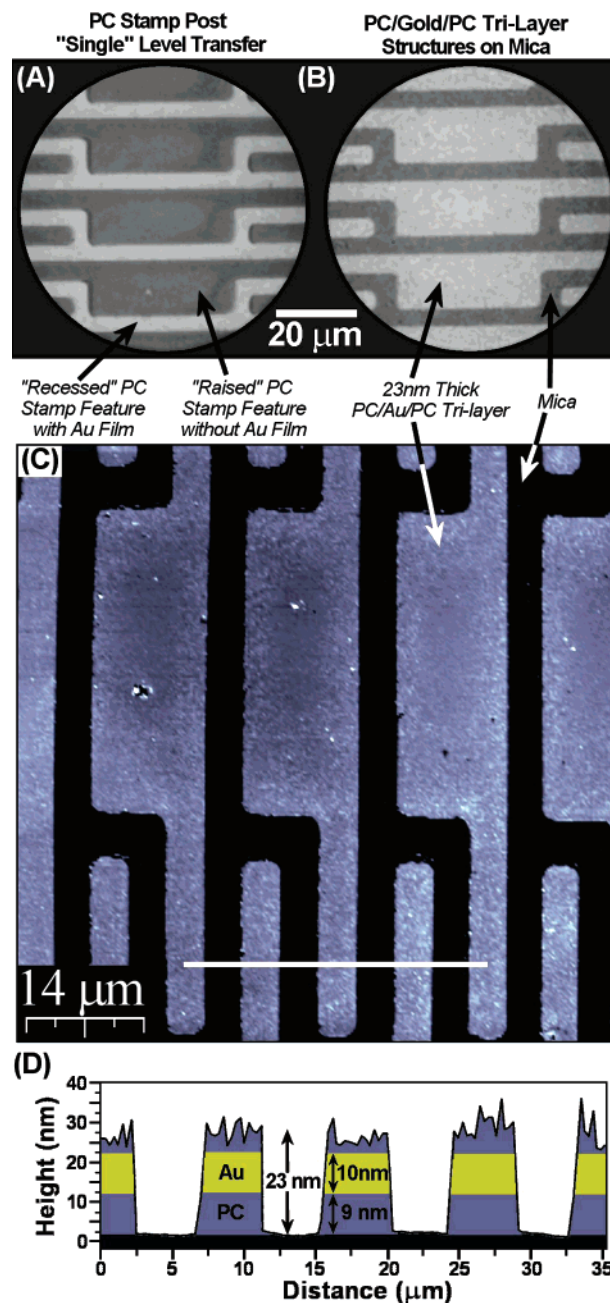


Figure 2. PMP₁ trilayer (PC/Au/PC) microstructures fabricated on mica using a compression molded Lexan PC stamp coated with 10 nm of Au. Fabrication was conducted at $145 \text{ }^\circ\text{C}$ for 1 min under an applied pressure of 0.85 MPa . (a) Optical micrograph of the PC stamp post-single-level transfer. Here the recessed stamp features continue to possess the Au film, while the Au film that resided on the raised stamp features is noticeably absent. (b) Optical micrograph of the single-level PMP₁ structures on mica. (c) AFM topography micrograph of the trilayer structures possessing a total height of $23 \pm 3.4 \text{ nm}$. Etching of the Au layer (which also removes the PC capping layer) reveals an interlayer thickness of $9 \pm 2 \text{ nm}$. From this we estimate the capping layer thickness to be ca. 4 nm .

Figure 2a is an optical image of the bilevel PC stamp postprocessing and illustrates that the Au film has been transferred solely from the *raised* stamp feature to the mica substrate. The resulting PMP₁ microstructures, given in the optical (Figure 2b) and AFM topography (Figure 2c and d) images, illustrate uniform pattern transfer for micron-scaled structures with processing times less than 10 min. Topography measurements (Figure 2d) reveal a total height of the PMP₁

(74) Vermaak, J. S.; Kuhlmann-Wilsdorf, D. *J. Phys. Chem.* **1968**, *72*, 4150–4154.

(75) Mays, C. W.; Vermaak, J. S.; Kuhlmann-Wilsdorf, D. *Surface Science* **1968**, *12*, 134–140.

(76) Burkstrand, J. M. *J. Appl. Phys.* **1981**, *52*, 4795–4800.

(77) *Eur. Phys. J. E* **2002**, *8*, 101–261.

(78) Li, D.; Han, B.; Huo, Q.; Wang, J.; Dong, B. *Macromolecules* **2001**, *34*, 4874–4878.

(79) Maeda, N.; Norisuye, T. *Polymer* **1993**, *34*, 3475–3480.

trilayer to be $\sim 23 \pm 3.4$ nm. Subsequent etching⁴¹ of the Au film layer ($h_{\text{Au}} = 10$ nm, RMS roughness ~ 1.1 nm), which also removes the PC capping layer, exposes the PC interlayer and reveals an interlayer thickness of $h_{\text{interlayer}} \sim 9$ nm ± 2 nm. Taking the difference therefore provides an estimate of $h_{\text{cap}} \sim 4$ nm for the mean capping layer thickness. Notably, the interlayer and capping layer thicknesses are comparable to the “dead” layer persistence lengths (~ 4 – 13 nm) extracted from thin film studies of polycarbonate.⁶⁹ A general and unexpected observation is the ability to fabricate PMP structures at temperatures well below a polymer's bulk T_g . For example, pattern transfer has been achieved at temperatures as low as 100 °C for Lexan polycarbonate, which is ~ 51 °C below its T_g of 151 °C. Such a finding supports the importance of ultrathin film phenomena in the described multilayer thermal nanotransfer technique, considering that the metal film acts as a physical barrier (Au films ≥ 10 nm) that obstructs penetration of the polymer into the Au–mica interface, and thereby requires a considerable amount of polymer diffusion in order to form the interlayer. Although the presented technique employs a loaded contact, such results lend credence to the presence of a mobile liquidlike interfacial polymer layer (i.e., precursor film⁸⁰) that spreads even at sub- T_g processing temperatures. Our findings further imply that the unique dynamics of the interfacial polymer chains are accompanied with a discernible change in the polymer's interfacial (adhesive and cohesive) properties. In fact, it has been suggested, from modeling of unentangled polycarbonate on a nickel surface, that interfacial polymer segregation could compromise cohesion between the adsorbed (“dead”) and adjacent bulklike macromolecules.⁸¹

Single-Level Transfer: PMP₁ Microstructure Fabrication with Optical Media. Commercially available polycarbonate compact disks (CDs) and digital video disks (DVDs), possessing a rectangular grating structure (Figure 1d) with a recess depth ~ 150 – 200 nm have also been employed as stamps for multilayer thermal nanotransfer of polymer–metal heterostructures. Procedures for the preparation of CD and DVD stamps were previously described⁴¹ and are also available in the Supporting Information. The single-level transfer products of Figure 3 were fabricated on mica with a Au-coated (15 nm) CD stamp. Topographic imaging (Figure 3a) reveals that the PMP₁ trilayer height is ~ 27 nm (excluding the prominent, ~ 85 nm, polymer edge feature). A serrated structure is evident in the SEM image (Figure 3b) and corresponds to the ledge in the topography profile (Figure 3c). The ledge is thought to arise from incomplete spreading or dewetting and/or an asymmetric fracture of the capping layer on the gold film during fabrication. Assuming that the ledge nominally corresponds to the top of the gold film surface, then the measured thickness of the capping layer is ~ 8 nm and the inferred thickness of the polymer interlayer is $h_{\text{interlayer}} \sim 4$ nm. This estimated thickness of the interlayer serves as an *upper limit*, considering that a finite capping layer (perhaps on the order of the Au film RMS roughness ~ 1.2 nm) may indeed exist on the ledge.⁸⁰ The difference between the interlayer heights measured for the structures of Figure 2 and Figure 3 may arise from several factors including differences in stamp composition (e.g., the presence of glass fillers in the CD stamps and differences in

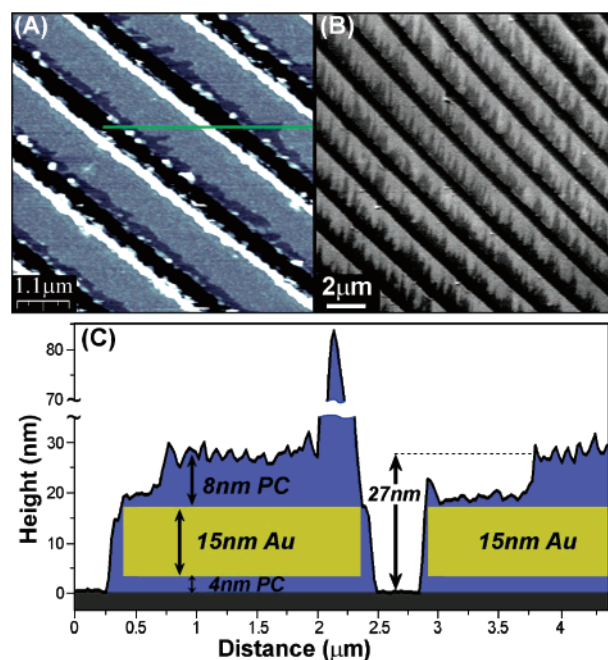


Figure 3. PMP₁ trilayer (PC/Au/PC) microstructures fabricated on mica using a bilevel polycarbonate compact disk (CD) stamp coated with 15 nm of Au. Fabrication was conducted at 145 °C for 10 min under an applied pressure of 1.3 MPa. (a) AFM topography and (b) SEM micrograph of the multilayered structures on mica. (c) The trilayer structures possess a total height of ~ 27 nm as illustrated in the AFM topography profile. Incomplete spreading, dewetting, or fracture of the capping layer leads to the serrated pattern in the SEM image and a ledge in the topography. The capping layer thickness is estimated from this ledge to be $h \sim 8$ nm, which provides an upper limit for the thickness of the polymer interlayer ($h \sim 4.2$ nm) considering that a finite capping layer may exist on “exposed” areas as depicted in the profile.

molecular weight or the polymer). As illustrated by the different processing parameters used to form the PMP heterostructures from gold-coated PC (e.g., temperature, soak time, and pressure), the physical properties of the polymer (e.g., M_w , surface energy, and dopants) have a significant effect on pattern fidelity, surface morphology, and trilayer thickness.

Using Lexan as the thermoplastic polymer stamp results in products with greater coverage and pattern fidelity than the products generated with optical recording media. While CDs and DVDs provide access to inexpensive stamps, high fidelity structures using these stamps are generally limited to numerous small domains (< 2 mm²) within the patterned region (0.5 – 2.5 cm²). Defect structures and incomplete structures are instructive as they reveal information about the potential resolution achievable with this approach and reveal information about the mechanism. For instance, some of the defective structures are noteworthy as they result in PMP₁ structures possessing lateral dimensions smaller than the defining relief structure of the stamp. Incomplete multilayer formation with this characteristic is observed and appears as an edge effect where local pressure gradients and/or poor contact parallelism lead to the formation of locally asymmetric stamp–surface contacts and polymer diffusion. This effect is clearly illustrated in the AFM (Figure 4a–c) and SEM (Figure 4d) images of the PMP₁ structures fabricated on mica with gold-coated CD stamps. Completed wires should possess a line width of ~ 1 μm, such as the case in Figure 4a, corresponding to the CD raised stamp feature width. As shown in Figure 4b–d, edge transfer effects yield

(80) Glick, D.; Thiansathaporn, P.; Superfine, R. *Appl. Phys. Lett.* **1997**, *71*, 3513–3515.

(81) Abrams, C. F.; Site, L. D.; Kremer, K. *Phys. Rev. E* **2003**, *67*, 021807.

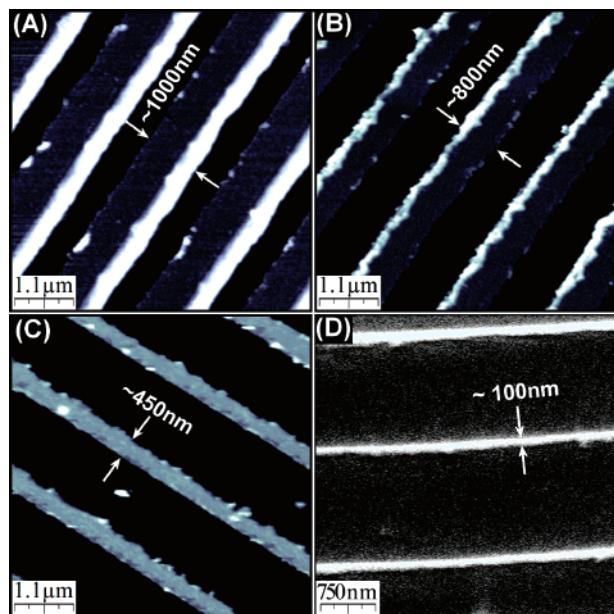


Figure 4. Various PMP_I trilayer (PC/Au/PC) microstructures fabricated on mica using Au-coated CD stamps. AFM topography images (a–c) and SEM micrograph (d) illustrate an edge transfer effect where incomplete multilayer formation can yield structures with a line width that is smaller than the 1 μm width of the raised CD stamp feature. Structures in (a) are consistent with the stamps raised feature width, while the (b–d) features are of varied completeness. The smallest line width of roughly 100 nm illustrates the current resolution capabilities of this technique.

wires with a range of widths, or equally, a varying degree of completion. Currently, the smallest feature widths generated with this edge effect are ~100 nm (Figure 4d), corresponding to a width reduction of ~10 times relative to the stamp relief dimension. This observation gives insight into the potential resolution the thermal nanolithography of polymer–metal heterostructures can achieve with the appropriate nanostructured polymer stamp.

Multilevel Transfer: PMP_{II} Nanostructure Fabrication with Optical Media. The second main multilayered product corresponds to the “multilevel” PMP_{II} array, depicted in Figure 1c, where materials are simultaneously transferred from both stamp levels, i.e., from *both* the raised “level I” and recessed “level II” features. The low- and high-resolution topography images of Figure 5a and b show a mixed array comprised of the level I and level II structures fabricated on mica with a bilevel DVD stamp (Figure 1d) coated with a 15 nm Au film. Single-level PMP_I structures, where transfer occurs only from the raised stamp features, are the exclusive product present in the lower right corner of the images. However, PMP_{II} structures, where transfer occurs from both the raised and recessed stamp features, predominate in the upper left corner. Comparatively, the level I and level II structures possess mean heights of 24 and 45 nm, respectively. This height variation is found to arise from a thickness variation in the capping layer, as the interlayer thickness ($h \sim 5$ nm) appears equivalent for both structures from etching and nanoshaving experiments. The detailed mechanism leading to similar interlayer heights for both level I and II structures is not understood but must arise from the Au and substrate surface energies, which are the principle drivers of interlayer formation, coupled with polymer reorganization and stamp deformation mechanics. Here the mean capping layer thickness for the level II structures ($h_{\text{cap}}^{\text{recessed}} \sim 25$ nm) is

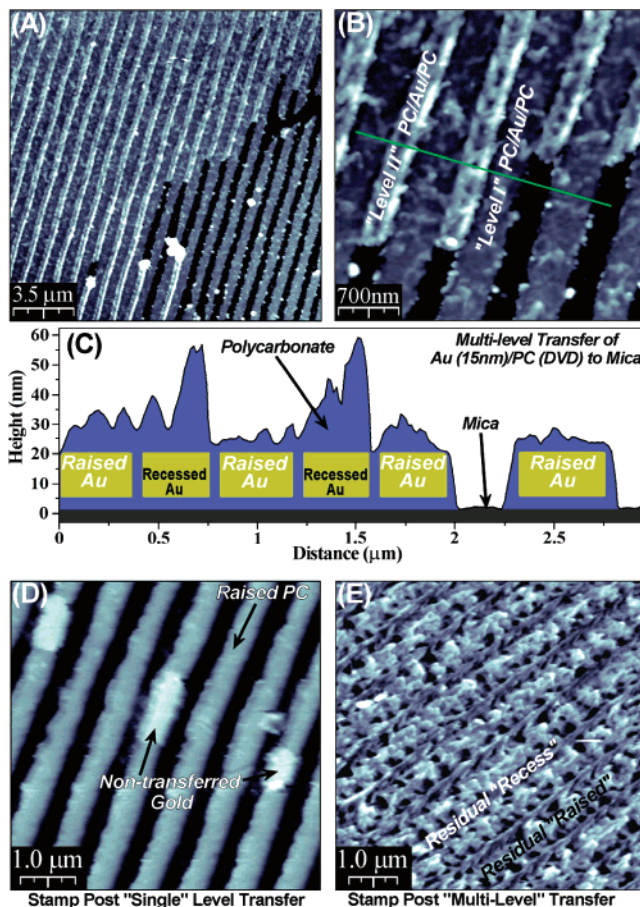


Figure 5. AFM topography images of PMP_{II} “multilevel” structures fabricated on mica using a polycarbonate (DVD) stamp coated with 15 nm of Au. Fabrication was conducted at 140 °C for 2 min under an apparent applied pressure of 3 MPa. (a and b) Low- and high-resolution topography images of the trilayer structures transferred from the raised and recessed stamp features (as labeled in Figure 5b). (c) AFM profile of the PMP_{II} structures where the raised and recessed structures possess a mean height of ~23 and 45 nm, respectively. An interlayer thickness $h \sim 5$ nm was measured for both the raised and recessed trilayer structures. The capping layer thickness is noticeably larger for the recessed structures ($h_{\text{cap}}^{\text{recessed}} \sim 25$ nm) than the raised structures ($h_{\text{cap}}^{\text{raised}} \approx 4$ nm \approx RMS roughness). (d) Topography image of the DVD stamp post “single” level transfer with the raised and recessed features clearly represented. A decrease in the raised feature height from 150 to 90 nm is observed. Portions of the Au film that have not been transferred to mica and are retained by raised stamp features are also noted. (e) Topography image of the DVD stamp post-“multilevel” transfer. The stamp is devoid of its initial grating structure and is nearly planarized with an RMS roughness of 13 nm.

appreciably larger than the thickness of the level I structure ($h_{\text{cap}}^{\text{raised}} \sim 5$ nm). This distinct topology is most often found near the boundary of the two product regimes (e.g., Figure 5). However, at the center of the PMP_{II} array (Supporting Information, Figure S7), the transition between the two surface structures is more subtle and is taken to be representative of the equilibrated PMP_{II} architecture, *vide infra*.

Inspection of the DVD stamps post single-level transfer (Figure 5d) reveals that although the raised and recessed features are clearly represented, there are noticeable topological changes. Most evident is the inelastic deformation of the stamp, where the relative feature height is found to decline from ~150 nm to ~90 nm. Also readily observed in this topography image are portions of the Au film that were not transferred to the substrate (Figure 5d). In contrast to the morphology after single-level

transfer, AFM imaging of the DVD stamp post-multilevel transfer (Figure 5e) reveals a topology that is markedly different in that the stamp is essentially devoid of its initial grating structure and is nearly planarized, with an RMS roughness of only ~ 13 nm. Strikingly, a complex “residual” morphology is observed on the stamp after multilevel transfer, which gives access to the initial stamp feature position and may also provide information about the processes active during this procedure. The details of the plastic yield mechanics and rheology associated with PMP_{II} structure fabrication are central to the further development of this aspect of the technique.

The plane projection of both stamp levels to the substrate is one of the most attractive aspects of the PMP_{II} arrays, as it enables generation of the small gap that separates the level I and level II structures. Previous work by Rogers et al. also illustrated the utility of a compliant polymer stamp step-edge (phase edge) by beneficially employing it in near-field phase shift lithography.⁸² In the work described herein, the fabricated multilevel heterostructures possess a level I and level II separation distance comparable to the former work. SEM imaging within the center region of a PMP_{II} array reveals a separation of ca. 100 nm (Supporting Information Figure SI 7A). Sample charging during image acquisition precludes a more detailed examination of this interface with SEM. From the AFM images (Figure SI 7b) the estimated structure gap of ca. 65 nm is consistent with SEM measurements. As previously mentioned, the topology of PMP_{II} structures vary from the center to the periphery (Figure 5). At the center, AFM imaging shows an array with a prominent polymer edge feature that is similar to that found in the PMP_I arrays of Figures 3 and 4. In general, these large edge structures are more frequently observed in the products from DVD and CD stamps while less frequently with Lexan stamps. As noted above, a likely cause of the topological differences between the Lexan polycarbonate and the recording media may be attributed to the differences in composition (e.g., glass fillers in the latter).

In conclusion, we have presented a new technique, which enables the fabrication of a multiplicity of polymer–metal–polymer, PMP, heterostructures on ceramic substrates in one thermal stamping process. These PMP structures are essentially polymer-coated metal wires where the metal arrays are insulated from each other and from the substrate. The multilayer thermal nanotransfer of polymer–metal heterostructures uses inexpensive, metal-coated thermoplastic stamps, is straightforward to implement, and is capable of fabricating ultrathin PMP architectures that range from microns to the nanoscale regime. This

readily accessible method provides a means of fabricating dense PMP arrays with sub-100 nm feature spacing and/or with different micro/nanowire widths. The batch-to-batch reproducibility for the thermal nanolithography of polymer–metal heterostructures is good when using the same processing conditions, the same polymer/gold/substrate compositions, and the same stamp structures; i.e., the PMP products have the same morphologies, defect densities, and the same surface coverage. Thus for a given system the technique is robust. Of particular importance is the occurrence of shear deformation during processing and the deleterious effects it has on structure continuity and fidelity. Such effects become most prevalent under higher processing temperatures (for example >140 °C with Lexan polycarbonate stamps) and represent an important parameter in future efforts to maximize structure fidelity with the single use stamps (batch mode processing) described herein.

Since many metal wires, polymers, or substrates are incompatible with chemical etchants, this multilayer thermal nanotransfer method expands the possible materials that can be used in nanofabrication of functional structures.^{83,84} The polymer interlayer formed between the nanowire and the substrate is generally less than 13 nm and is a result of thermodynamic self-organization of the polymer into the metal–substrate interface during the stamping process. Special tooling is not required with this technique nor does it require advanced material formulations, as readily available CD, DVD, and Lexan polycarbonate stamps have been used to demonstrate this technique. In contrast to many stamping methods, the fabrication of smaller nanoscaled PMP products occurs with greater structural fidelity and greater yield in terms of coverage than using the same materials and conditions to produce micron scaled features.

Acknowledgment. We gratefully acknowledge support from the National Science Foundation (IGERT DGE–9972892, and CHE-0554703 to C.M.D.) and the Israel-U.S. Binational Science Foundation to C.M.D. An Irving Hochberg Dissertation Fellowship in the Sciences, the Graduate Center of the City University of New York to J.M.H. is acknowledged. We also thank Donald Helt Sr. for access to the machining facilities and his assistance in fabrication of the UV-ozone cleaner and compression cell. We thank Prof. William L’Amoreaux (CUNY-CSI) for his continued assistance with the SEM and Prof. James D. Batteas (Texas A&M) for suggestions and reading the manuscript.

Supporting Information Available: Sample and stamp preparation methods, further information on the mechanism, and a description of patterning parameters. This material is available free of charge via the Internet at <http://pubs.acs.org>.

JA056809Z

(82) Rogers, J. A.; Paul, K. E.; Jackman, R. J.; Whitesides, G. M. *Appl. Phys. Lett.* **1997**, *70*, 2658–2660.

(83) Ozbay, E. *Science* **2006**, *311*, 189–193.

(84) Ioannidis, A.; Facci, J. S.; Abkowitz, M. A. *J. Appl. Phys.* **1998**, *84*, 1439–1444.